



**HAL**  
open science

## Solvent- and Halide-Induced (Inter)conversion between Iron(II)-Disulfide and Iron(III)-Thiolate Complexes

Lianke Wang, Fabián Cantú reinhard, Christian Philouze, Serhiy Demeshko, Sam De visser, Franc Meyer, Franc Gennari, Franc Duboc

► **To cite this version:**

Lianke Wang, Fabián Cantú reinhard, Christian Philouze, Serhiy Demeshko, Sam De visser, et al.. Solvent- and Halide-Induced (Inter)conversion between Iron(II)-Disulfide and Iron(III)-Thiolate Complexes. *Chemistry - A European Journal*, 2018, 24 (46), pp.11973-11982. 10.1002/chem.201801377 . hal-02048074

**HAL Id: hal-02048074**

**<https://hal.science/hal-02048074v1>**

Submitted on 15 Dec 2024

**HAL** is a multi-disciplinary open access archive for the deposit and dissemination of scientific research documents, whether they are published or not. The documents may come from teaching and research institutions in France or abroad, or from public or private research centers.

L'archive ouverte pluridisciplinaire **HAL**, est destinée au dépôt et à la diffusion de documents scientifiques de niveau recherche, publiés ou non, émanant des établissements d'enseignement et de recherche français ou étrangers, des laboratoires publics ou privés.



# Solvent- and halide- induced (inter)conversion between iron(II)-disulfide and iron(III) thiolate complexes

**DOI:**

[10.1002/chem.201801377](https://doi.org/10.1002/chem.201801377)

**Document Version**

Accepted author manuscript

[Link to publication record in Manchester Research Explorer](#)

**Citation for published version (APA):**

Wang, L., Cantu Reinhard, F., Philouze, C., Demeshko, S., De Visser, S., Meyer, F., Gennari, M., & Duboc, C. (2018). Solvent- and halide- induced (inter)conversion between iron(II)-disulfide and iron(III) thiolate complexes. *Chemistry: A European Journal*, 24(46), 11973-11982. <https://doi.org/10.1002/chem.201801377>

**Published in:**

Chemistry: A European Journal

**Citing this paper**

Please note that where the full-text provided on Manchester Research Explorer is the Author Accepted Manuscript or Proof version this may differ from the final Published version. If citing, it is advised that you check and use the publisher's definitive version.

**General rights**

Copyright and moral rights for the publications made accessible in the Research Explorer are retained by the authors and/or other copyright owners and it is a condition of accessing publications that users recognise and abide by the legal requirements associated with these rights.

**Takedown policy**

If you believe that this document breaches copyright please refer to the University of Manchester's Takedown Procedures [<http://man.ac.uk/04Y6Bo>] or contact [uml.scholarlycommunications@manchester.ac.uk](mailto:uml.scholarlycommunications@manchester.ac.uk) providing relevant details, so we can investigate your claim.



**Solvent- and halide- induced (inter)conversion between  
iron(II)-disulfide and iron(III) thiolate complexes**

Lianke Wang,<sup>a</sup> Fabian G. Cantú Reinhard,<sup>b</sup> Christian Philouze,<sup>a</sup> Serhiy Demeshko,<sup>c</sup> Sam P. de Visser,<sup>b</sup> Franc Meyer,<sup>c</sup> Marcello Gennari,<sup>a\*</sup> Carole Duboc<sup>a\*</sup>

<sup>a</sup> *Université Grenoble Alpes, UMR CNRS 5250, Département de Chimie Moléculaire, F-38000 Grenoble, France*

<sup>b</sup> *Manchester Institute of Biotechnology and School of Chemical Engineering and Analytical Science, The University of Manchester, 131 Princess Street, Manchester M1 7DN, United Kingdom*

<sup>c</sup> *Institute of Inorganic Chemistry, Georg-August-University Göttingen, Tammannstrasse 4, D- 37077 Göttingen, Germany*

\* corresponding authors. [carole.duboc@univ-grenoble-alpes.fr](mailto:carole.duboc@univ-grenoble-alpes.fr),  
[marcello.gennari@univ-grenoble-alpes.fr](mailto:marcello.gennari@univ-grenoble-alpes.fr)

## Abstract

Disulfide/thiolate interconversion controlled by copper is proposed to be involved in relevant biological processes, such as copper delivery and protection of cells against reactive oxygen species. In analogy to copper, it can be envisaged that iron also participates in the control of similar biological processes. We describe herein iron complexes that undergo  $\text{Fe}^{\text{III}}$ -thiolate/ $\text{Fe}^{\text{II}}$ -disulfide (inter)conversion mediated not only by halide (de)coordination as in the previously reported parent cobalt and manganese complexes, but also by the nature of the solvent. The dinuclear  $\text{Fe}^{\text{II}}$ -disulfide complex  $[\text{Fe}^{\text{II}}_2(\text{LSSL})]^{2+} ((\text{LS})^{2-} = 2,2'-(2,2'-\text{bipyridine-6,6'-diyl})\text{bis}(1,1\text{-diphenylethanethiolate}), (\text{LSSL})^{2-}$ , the corresponding disulfide ligand) shows solvent-dependent properties: while in non-coordinating solvent (dichloromethane), the dinuclear  $\text{Fe}^{\text{II}}$ -disulfide complex is the only stable form. In the presence of coordinating solvents like acetonitrile or DMF, it is partly or fully converted into mononuclear  $\text{Fe}^{\text{III}}$ -thiolate species having a bound solvent molecule  $([\text{Fe}^{\text{III}}(\text{LS})(\text{Solv})]^+$ ,  $\text{Solv} = \text{DMF}, \text{MeCN}$ ). Addition of chloride to a dichloromethane solution containing the  $\text{Fe}^{\text{II}}$ -disulfide dinuclear complex leads to the fast and quantitative formation of a mononuclear  $\text{Fe}^{\text{III}}$ -thiolate species with a bound chloride, i.e.  $([\text{Fe}^{\text{III}}(\text{LS})\text{Cl}]$ ). The reverse reaction can be achieved by addition of  $\text{Li}[[\text{B}(\text{C}_6\text{F}_5)_4]$ . In relation to the metal-sulfur electronic distribution, the comparison between the redox properties of the Fe, Mn and Co complexes involved in these  $\text{M}^{\text{III}}$ -thiolate/ $\text{M}^{\text{II}}$ -disulfide interconversion processes allows rationalizing their respective efficiency.

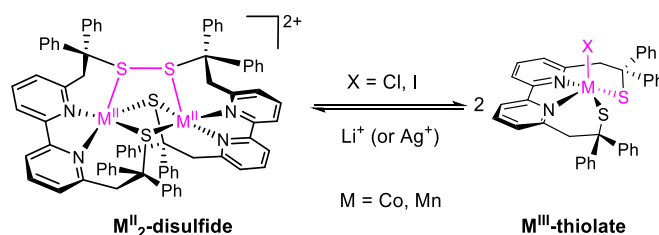
## Introduction

Sulfur-containing compounds, especially those including cysteine, glutathione or thioredoxin that are known to be prone to thiolate/disulfide interconversion processes, are largely found in different cellular compartments where they act as structural and chemical transducing agents.<sup>[1]</sup> The fine-tuning of the equilibrium potential<sup>[2]</sup> in each cellular space affects the relative concentration of the oxidized and reduced forms of these molecules and thus have an impact on the specific chemical organization and function of each cellular compartment. Transition metal ions can participate and assist in the control of this thiolate/disulfide (inter)conversion, and particularly copper is often found. Such process has been proposed to be involved in the formation of copper-based biological active sites,<sup>[3]</sup> as the  $\text{Cu}_A$ , or in the control of the concentration of reactive oxygen species (ROS).<sup>[4]</sup> For a better understanding of the factors that govern such copper-based thiolate/disulfide (inter)conversion, chemists have characterized different  $\text{Cu}^{\text{I}}$ -disulfide/ $\text{Cu}^{\text{II}}$ -thiolate switches with conversion processes controlled by temperature,<sup>[5]</sup> solvent polarity,<sup>[5]</sup> acidic-basic conditions<sup>[6]</sup> or (de)coordination of chloride.<sup>[7]</sup> More recently, we have extended this family of copper-based systems to isostructural cobalt- and manganese-based complexes that display  $\text{M}^{\text{II}}$ -disulfide/ $\text{M}^{\text{III}}$ -thiolate

interconversion processes mediated by (de)coordination of halides.<sup>[8]</sup> In the presence of chloride or iodide, the dinuclear  $M^{II}$ -disulfide complexes ( $M = Co$  and  $Mn$ ; Scheme 1) are converted into the corresponding mononuclear  $M^{III}$ -thiolate species that contains one coordinated halide. Binding of the halide to the metal promotes an internal electron transfer from the metal ion to the disulfide moiety, i.e. the reduction of the disulfide into two thiolates, combined with metal oxidation. Inversely, the release of the halide provokes the oxidation of thiolates to disulfide accompanied by metal reduction. Controlling such a process is challenging to predict since it depends on several factors including the covalency of the metal-sulfur bond and the redox properties of the complexes.

In the present work, our objective was to enlarge this investigation on metal-promoted thiolate/disulfide interconversion to iron, which represents together with copper the most abundant redox active metal in biological media. Iron-sulfur complexes are broadly present in biology as electron transfer agents ( $[Fe-S]$  clusters),<sup>[9]</sup> or in the active sites of enzymes involved in the reduction of small molecules such as hydrogenases,<sup>[10]</sup> CO dehydrogenases<sup>[11]</sup> or nitrogenases.<sup>[12]</sup> Iron is also proposed to be involved in the production and destruction of ROS.<sup>[13]</sup> Similarly to the case of copper, iron-controlled thiolate/disulfide interconversion is potentially involved in cellular iron delivery processes and in the regulation of ROS concentration. In addition, a thiolate/disulfide switch has been proposed to be directly implicated in the reaction mechanism of iron-containing nitrile hydratase.<sup>[14]</sup>

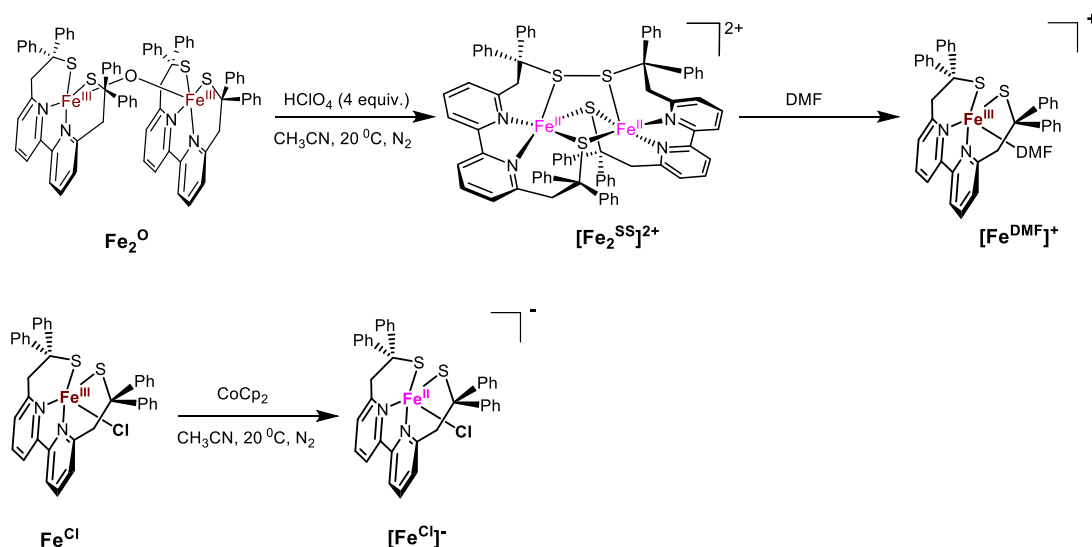
We describe herein iron complexes isostructural to the previously described Co and Mn derivatives, which undergo thiolate/disulfide conversion mediated by halide (de)coordination. A comparison between the redox properties of the complexes involved in the interconversion process allows to rationalize the different switching efficiency of the cobalt, manganese and iron systems. We also found that, even in the absence of halides, the relative stability of the  $Fe^{II}$ -disulfide and  $Fe^{III}$ -thiolate forms is strongly influenced by the nature of the solvent.



**Scheme 1.** Schematic representation of the interconversion between reported  $M^{II}$ -disulfide and  $M^{III}$ -thiolate complexes.

## Results

**Synthesis and solid state characterization.** All the complexes described and/or discussed in the text are depicted in Scheme S2, while the corresponding ligands,  $H_2(LS)$  and  $H_2(LSSL)$ , are shown in Scheme S1. The perchlorate salt of the  $Fe^{II}$ -disulfide  $[Fe^{II}_2(LSSL)]^{2+}$  complex ( $[Fe_2^{SS}]^{2+}$ ) was isolated as an orange precipitate by protonation of the previously reported  $\mu$ -oxo complex  $[Fe^{III}_2(LS)_2(\mu-O)]$  ( $[Fe_2^O]^{15}$ ) via addition of a two-fold excess of  $HClO_4$  (4 equiv. vs oxo) in acetonitrile (Scheme 2).



**Scheme 2.** Synthesis of  $[Fe_2^{SS}]^{2+}$ ,  $[Fe^{DMF}]^+$  and  $[Fe^{Cl}]^-$ .

Single-crystals of the product were grown by slow diffusion of diethyl ether into the acetonitrile mother liquid. The corresponding X-ray structure reveals a  $\mu_{1,2}-\eta^1:\eta^1$ -disulfide bis( $\mu$ -thiolate) dinuclear  $Fe^{II}$  complex containing a  $\{Fe_2S_2(SS)\}$  core, as displayed in Figure 1a (selected distances are given in Table 1). Such a core is relatively rare in coordination chemistry and unprecedented for iron complexes (if only organic disulfides are considered, with the exclusion of the  $S_2^{2-}$  anion). The  $[Fe_2^{SS}]^{2+}$  complex is isostructural to the previously reported  $Co^{[8a]}$  and  $Mn^{[8b]}$  derivatives ( $[Co_2^{SS}]^{2+}$  and  $[Mn_2^{SS}]^{2+}$ , respectively) and similarly it displays a quasi-planar  $\{Fe_2S_2\}$  core (less than  $0.094 \text{ \AA}$  deviation from the mean plane formed by  $Fe1S2Fe1'S2'$ ,  $13.88^\circ$  angle between the  $S2Fe1S2'$  and  $S2Fe1'S2'$  planes). The disulfide remains coordinated to both Fe atoms in a *cis*- $\mu$ -1,2 mode. The short  $S2-S2'$  distance of  $2.0233(16) \text{ \AA}$  is typical of a disulfide bond and is similar to that found in the reported Co and Mn complexes ( $2.0243(13)$  and  $2.0357(17) \text{ \AA}$ , respectively). The long  $Fe^{III}-Fe$  distance of  $3.095 \text{ \AA}$  implies the absence of direct metal-metal interaction. The Fe sites are equivalent because of a  $C_2$  symmetry axis that is orthogonal to the mean  $\{Fe_2S_2\}$  plane. The  $N2S3$  coordination sphere around each  $Fe^{II}$  center displays a distorted square pyramidal geometry with a  $\tau_5$  value of  $0.12$  similar to the Mn and Co derivatives ( $\tau_5$  values of  $0.07$  and  $0.13$ ,

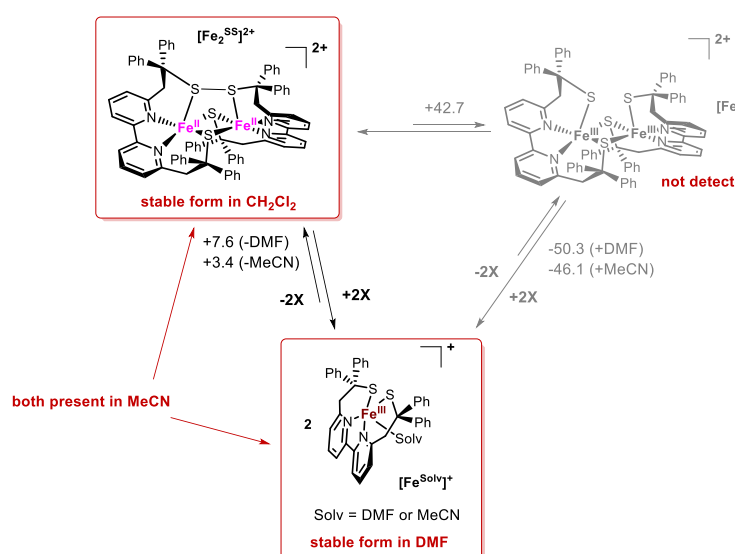
respectively). More specifically, the plane is formed by two N atoms of the bipyridine unit of one L<sup>N2S2</sup> ligand and two bridging S atoms from thiolates, while the axial position is occupied by one S atom of the disulfide bridge. Due to the weaker donor ability of disulfide vs thiolate, the axial Fe<sup>II</sup>-S<sub>S,S</sub> bond (2.5513(9) Å) is significantly longer than the basal Fe<sup>II</sup>-S<sub>thiolate</sub> bonds (2.4131(9) and 2.3641(10) Å). All the iron-related bond lengths are slightly longer than those in [Co<sub>2</sub><sup>SS</sup>]<sup>2+</sup> and shorter than in [Mn<sub>2</sub><sup>SS</sup>]<sup>2+</sup>, which is in agreement with the periodic trend. The +II oxidation state of the Fe ions has been confirmed by the powder zero-field <sup>57</sup>Fe Mössbauer spectrum of [Fe<sub>2</sub><sup>SS</sup>]<sup>2+</sup> recorded at 80 K (Figure 2a). It displays a quadrupole doublet with an isomer shift  $\delta = 0.91 \text{ mm s}^{-1}$  and a quadrupole splitting  $\Delta E_Q = 3.62 \text{ mm s}^{-1}$ , corresponding to the main feature (89%). The  $\delta$  value is consistent with two identical high-spin ferrous ( $S = 2$ ) ions. Despite several trials (synthesis and purification procedures), the isolated complex invariably contains a minor Fe-based impurity that was not unambiguously identified.

Black single crystals of the Fe<sup>III</sup>-thiolate DMF adduct [Fe<sup>III</sup>(LS)(DMF)]<sup>+</sup> ([Fe<sup>DMF</sup>]<sup>+</sup>, perchlorate form) have been isolated when dissolving the Fe<sup>II</sup>-disulfide complex [Fe<sub>2</sub><sup>SS</sup>]<sup>2+</sup> in N,N-dimethylformamide after slow diffusion of diethyl ether. X-ray diffraction data demonstrate the mononuclear structure of the adduct (Figure 1b, Table 1). The five-coordinated iron center displays a distorted square pyramidal geometry ( $\tau_5$  value of 0.29) with a N<sub>2</sub>S<sub>2</sub>O coordination sphere. The oxygen atom from DMF occupies the apical position, while the two N and two S atoms of the tetradentate ligand are located in the equatorial plane. The iron center resides approximately 0.484 Å out of the mean equatorial plane towards the axial oxygen from DMF (vs 0.531 Å for the reported [Fe<sup>III</sup>(LS)Cl] complex, Fe<sup>Cl</sup>).<sup>[15]</sup> The zero-field <sup>57</sup>Fe Mössbauer spectrum of [Fe<sup>DMF</sup>]<sup>+</sup> (80 K, Figure 2b) evidences the intermediate spin state ( $S = 3/2$ ) of the Fe<sup>III</sup> complex. Indeed, both the isomer shift ( $\delta = 0.41 \text{ mm s}^{-1}$ ) and the quadrupole splitting ( $\Delta E_Q = 3.09 \text{ mm s}^{-1}$ ) of the observed doublet are close to the parameters reported for the intermediate spin state Fe<sup>III</sup>-halide complexes [Fe<sup>III</sup>(LS)X] (Fe<sup>X</sup>,  $\delta = 0.43, 0.42, 0.41 \text{ mm s}^{-1}$  and  $\Delta E_Q = 2.74, 2.82, 2.85 \text{ mm s}^{-1}$ , for X = Cl, Br, I, respectively).<sup>[16]</sup> The one-electron reduced form of [Fe<sup>III</sup>(LS)Cl] (Fe<sup>Cl</sup>) was prepared and isolated by addition of cobaltocene (CoCp<sub>2</sub>) to Fe<sup>Cl</sup> in acetonitrile solution. The single-crystal X-ray diffraction characterization of the [CoCp<sub>2</sub>]<sup>+</sup> form of the [Fe<sup>II</sup>L(Cl)]<sup>-</sup> complex ([Fe<sup>Cl</sup>]<sup>-</sup>, Figure 1c, Table 1) shows its mononuclear character and a quasi-perfect square pyramidal geometry around Fe, with  $\tau_5$  values of 0.032 / 0.005 (values are given for the two independent molecules present in the crystal). Its overall structural properties are similar to those of its reported oxidized form,<sup>[15]</sup> with the expected increase of all Fe-ligand bond distances. Concerning the Fe-Cl bond lengths, these distances are close in both complexes (2.306(3) and 2.3390(11)/2.3409(11) Å, respectively in Fe<sup>Cl</sup> and [Fe<sup>Cl</sup>]<sup>-</sup>). This is compensated by the different location of the iron center that resides approximately 0.480 Å and 0.716 Å, respectively, out of the mean N<sub>2</sub>S<sub>2</sub> plane towards the axial chloride ion. The zero-field <sup>57</sup>Fe Mössbauer spectrum of [Fe<sup>Cl</sup>]<sup>-</sup> (80 K, Figure 2c) displays a doublet with an isomer shift of 0.91 mm s<sup>-1</sup> and a quadrupole splitting of

4.15 mm s<sup>-1</sup> evidencing a high-spin state ( $S = 2$ ) for the mononuclear Fe<sup>II</sup> center.

**Solvent-dependent equilibria between Fe<sup>II</sup>-disulfide ([Fe<sub>2</sub><sup>SS</sup>]<sup>2+</sup>) and Fe<sup>III</sup>-thiolate ([Fe<sup>Solv</sup>]<sup>+</sup>) forms.** The isolation of [Fe<sup>DMF</sup>]<sup>+</sup> from the corresponding dinuclear Fe<sup>II</sup>-disulfide compound [Fe<sub>2</sub><sup>SS</sup>]<sup>2+</sup> in DMF (see above) suggests that Fe<sup>II</sup>-disulfide/Fe<sup>III</sup>-thiolate conversion process can occur in solution under particular conditions. The fact that one DMF molecule is coordinated in [Fe<sup>DMF</sup>]<sup>+</sup> indicates the main role of the solvent in driving the process and stabilizing the Fe<sup>III</sup>-thiolate form.

To gain further insight into the Fe<sup>II</sup>-disulfide/Fe<sup>III</sup>-thiolate conversion process, we thus investigated the speciation of [Fe<sub>2</sub><sup>SS</sup>]<sup>2+</sup> in solvents with different coordination abilities (dichloromethane, acetonitrile, N,N-dimethylformamide). These studies, supported by multiple experimental techniques in combination with DFT calculations, attest how in coordinating solvents the Fe<sup>II</sup>-disulfide complex is partly or totally converted into the corresponding mononuclear Fe<sup>III</sup>-thiolate form ([Fe<sup>Solv</sup>]<sup>+</sup>), while only [Fe<sub>2</sub><sup>SS</sup>]<sup>2+</sup> is stable in non-coordinating solvents (Scheme 3). The implication of the dinuclear Fe<sup>III</sup>-thiolate complex (named [Fe<sub>2</sub>]<sup>2+</sup>, see Scheme 3), an isoelectronic form of [Fe<sub>2</sub><sup>SS</sup>]<sup>2+</sup>, as an intermediate during the process is unlikely, since [Fe<sub>2</sub>]<sup>2+</sup> has been calculated to be 42.7, 50.3 and 46.1 kcal mol<sup>-1</sup> less stable than [Fe<sub>2</sub><sup>SS</sup>]<sup>2+</sup>, [Fe<sup>DMF</sup>]<sup>+</sup> and [Fe<sup>MeCN</sup>]<sup>+</sup>, respectively.



**Scheme 3.** Speciation of [Fe<sub>2</sub><sup>SS</sup>]<sup>2+</sup> in solution (CH<sub>2</sub>Cl<sub>2</sub>, MeCN, DMF), including the calculated relative energies (with zero-point and solvent corrections included in kcal mol<sup>-1</sup>, see Table S5). The calculated thermodynamics allow us to rule out the formation of a dinuclear Fe<sup>III</sup>-thiolate intermediate ([Fe<sub>2</sub>]<sup>2+</sup>, in grey).

The UV-vis spectrum of a CH<sub>2</sub>Cl<sub>2</sub> solution of [Fe<sub>2</sub><sup>SS</sup>]<sup>2+</sup> (Figure 3) with an absorption band at around 450 nm ( $\epsilon \approx 2700 \text{ L} \cdot \text{mol}^{-1} \cdot \text{cm}^{-1}$ ) is similar to that observed in the solid-state spectrum suggesting the preservation of the Fe<sup>II</sup>-disulfide complex in CH<sub>2</sub>Cl<sub>2</sub> solution. When [Fe<sub>2</sub><sup>SS</sup>]<sup>2+</sup>

is dissolved in MeCN or DMF, a much more intense band is observed in the same region (at 449 and 475 nm ( $\epsilon \approx 6800 \text{ L}\cdot\text{mol}^{-1}\cdot\text{cm}^{-1}$ ), respectively), which can be assigned to a charge transfer transition from thiolate to  $\text{Fe}^{\text{III}}$ .<sup>[17]</sup> Two weaker features also appear at lower energies (at 641 and 745 nm in MeCN and at 605 and 710 nm in DMF). Coherently, when a small amount of DMF (corresponding to 1% v/v) is added to a  $\text{CH}_2\text{Cl}_2$  solution of  $[\text{Fe}_2^{\text{SS}}]^{2+}$ , the progressive increase of the thiolate to  $\text{Fe}^{\text{III}}$  band at 475 nm and of the two weaker visible transitions is observed, the process being complete in approximately 50 min, as shown in Figure S1. The overall UV-vis data thus indicate the conversion of  $[\text{Fe}_2^{\text{SS}}]^{2+}$  into  $\text{Fe}^{\text{III}}$ -thiolate species in coordinating solvents like MeCN and DMF.

In agreement with UV-vis data, the ESI-mass spectrum of  $[\text{Fe}_2^{\text{SS}}]^{2+}$  in  $\text{CH}_2\text{Cl}_2$  further confirms the preservation of dinuclearity, since a +2 main peak is observed at 634.1  $m/z$  and a +1 peak is observed at 1367.1  $m/z$ , corresponding to  $[\text{Fe}_2(\text{LSSL})]^{2+}$  and  $[\text{Fe}_2(\text{LSSL})\text{ClO}_4]^+$ , respectively (Figure 4a). Conversely, the mass spectra in MeCN and DMF display a +1 main peak (at 634.1 and 706.9  $m/z$ , respectively) attributed to the mononuclear species,  $[\text{Fe}(\text{LS})]^+$  and  $[\text{Fe}(\text{LS})(\text{DMF})]^+$ , respectively (Figure 4b-c). **The absence of a mass-adduct in MeCN and its presence in DMF may reflect a poorer affinity of  $\text{Fe}^{\text{III}}$  for MeCN than for DMF.**

The presence of mononuclear  $\text{Fe}^{\text{III}}$  adducts in coordinating solvents has been confirmed by *cw* X-band EPR spectroscopy (Figure S2): in the spectra recorded at 100 K, an intense transition at  $g \approx 3.8$  has been observed in both MeCN and DMF, but not in  $\text{CH}_2\text{Cl}_2$ . This feature has been attributed to an  $S = 3/2$  ground spin state corresponding to a mononuclear intermediate spin  $\text{Fe}^{\text{III}}$  complex, analogous to the reported chloride adduct  $\text{Fe}^{\text{Cl}}$ .<sup>[15]</sup>

Finally, the analysis of the  $^1\text{H}$  NMR spectra of  $[\text{Fe}_2^{\text{SS}}]^{2+}$  dissolved in  $\text{CD}_2\text{Cl}_2$ ,  $\text{CD}_3\text{CN}$  and  $d_7$ -DMF allows for the supply of an overall picture of the speciation in these different solvents. All the spectra are paramagnetic, showing peak shifts in the NMR spectra that span from around +45 to -35 ppm (Figure 5). The  $^1\text{H}$  NMR spectrum in  $d_7$ -DMF displays three shifted resonances of equal intensity at  $\delta$  33.17 (1H), -1.08 (1H) and -26.44 (1H), a pattern very similar to that observed for  $\text{Fe}^{\text{Cl}}$ .<sup>[15]</sup> The longitudinal relaxation times ( $T_1$ , Table S3) are also comparable to those of  $\text{Fe}^{\text{Cl}}$ . This is a definitive confirmation of the presence of the mononuclear  $[\text{Fe}^{\text{DMF}}]^+$  complex as main species in DMF solution. In the same solvent, a  $\chi T = 1.71 \text{ cm}^3\cdot\text{K}\cdot\text{mol}^{-1}$  was determined by the Evans method,<sup>[18]</sup> which is in reasonable agreement with the presence of an  $S = 3/2$  state (spin-only value  $1.875 \text{ cm}^3\cdot\text{K}\cdot\text{mol}^{-1}$ ). The  $^1\text{H}$  NMR spectrum of  $[\text{Fe}_2^{\text{SS}}]^{2+}$  in  $\text{CD}_2\text{Cl}_2$  displays a completely different pattern, with at least thirteen paramagnetically shifted signals. By considering their relative intensities (see Table S3), all of these peaks are assigned to a single species. Taking into account the UV-vis, ESI-mass, EPR and X-ray diffraction data (see above), this species is assigned as the original  $[\text{Fe}_2^{\text{SS}}]^{2+}$  complex. Finally, the  $^1\text{H}$  NMR spectrum in  $\text{CD}_3\text{CN}$  solution clearly shows a mixture (in a ~1:2 ratio) of both the  $\text{Fe}^{\text{II}}$ -disulfide  $[\text{Fe}_2^{\text{SS}}]^{2+}$  complex and a mononuclear  $\text{Fe}^{\text{III}}$ -thiolate solvent adduct similar to  $[\text{Fe}^{\text{DMF}}]^+$  ( $[\text{Fe}^{\text{MeCN}}]^+$ ). The fact that the equilibrium between  $[\text{Fe}_2^{\text{SS}}]^{2+}$  and the corresponding solvent adduct  $[\text{Fe}^{\text{Solv}}]^+$  (Solv = MeCN or DMF) is less displaced

towards the mononuclear complex in MeCN than in DMF, is in agreement with the DFT-calculated thermodynamic parameters of both reactions ( $\Delta E = -3.4$  and  $-7.6$  kcal mol<sup>-1</sup> for X= MeCN and DMF, respectively, see Table S5). An additional minor species is also present in MeCN, whose peaks disappear under acidic conditions (addition of [LutH]BF<sub>4</sub>, [LutH]<sup>+</sup> = 2,6-lutidinium). This compound has been assigned to an hydroxo-containing/bridged Fe<sup>III</sup> complex [Fe<sup>III</sup><sub>2</sub>(LS)<sub>2</sub>(OH)]<sup>+</sup> ([Fe<sub>2</sub><sup>OH</sup>]<sup>+</sup>), formed by reaction of [Fe<sup>MeCN</sup>]<sup>+</sup> with water molecules that are present in CD<sub>3</sub>CN. This species can be also detected by ESI-MS (peak at 1285.3 *m/z*, Figure 4b) and CV (see below), and it is proposed to be similar to the previously reported Mn<sup>III</sup>-hydroxo adduct [Mn<sup>III</sup><sub>2</sub>(LS)<sub>2</sub>( $\mu$ -OH)]<sup>+</sup> ([Mn<sub>2</sub><sup>OH</sup>]<sup>+</sup>).<sup>[19]</sup>

DFT calculations have been performed to highlight the role of the solvent in this solvent-dependent equilibrium by understanding the electronic modifications induced by removing the solvent-bound molecule of the [Fe<sup>Solv</sup>]<sup>+</sup> complexes. The Mulliken spin population analysis performed on the DFT-optimized geometry of [Fe<sup>III</sup>(LS)]<sup>+</sup> (initiated from the X-ray data of [Fe<sup>DMF</sup>]<sup>+</sup> after removing the DMF molecule) evidences a notable increase of the spin population on the sulfur atoms in comparison to [Fe<sup>III</sup>(LS)Solv]<sup>+</sup> (0.23 for [Fe<sup>III</sup>(LS)]<sup>+</sup>, 0.08 for [Fe<sup>III</sup>(LS)MeCN]<sup>+</sup> and -0.04 for [Fe<sup>III</sup>(LS)DMF]<sup>+</sup>, see Table S7). The manifested thiol character of the thiolates leads to an increase of their reactivity and their likely conversion into a disulfide bridge between two [Fe<sup>III</sup>(LS)]<sup>+</sup> units to generate [Fe<sub>2</sub><sup>SS</sup>]<sup>2+</sup>.

**Redox properties of [Fe<sub>2</sub><sup>SS</sup>]<sup>2+</sup> and [Fe<sup>Solv</sup>]<sup>+</sup> (Solv = MeCN, DMF).** The redox properties of these three species have been examined by cyclic voltammetry (CV) of [Fe<sub>2</sub><sup>SS</sup>]<sup>2+</sup> dissolved in CH<sub>2</sub>Cl<sub>2</sub>, MeCN and DMF (Figure 6). The CH<sub>2</sub>Cl<sub>2</sub> solution displays a poorly reversible reduction process at  $E_{pc} = -0.84$  V vs Fc/Fc<sup>+</sup> ( $E_{pa} = -0.67$  V,  $i_{pa}/i_{pc} = 0.45$ ) that can be assigned to the two-electron reduction of the disulfide bridge of [Fe<sub>2</sub><sup>SS</sup>]<sup>2+</sup>.<sup>[8]</sup> By contrast, the CV in DMF solution shows a reversible cathodic process ( $E_{1/2} = -0.71$  V,  $\Delta E_p = 80$  mV,  $i_{pa}/i_{pc} = 0.94$ ), assigned to the Fe<sup>III</sup> → Fe<sup>II</sup> one-electron reduction in [Fe<sup>DMF</sup>]<sup>+</sup>. A similar fully reversible metal-based one-electron reduction process is observed in MeCN ( $E_{1/2} = -0.59$  V,  $\Delta E_p = 70$  mV,  $i_{pa}/i_{pc} = 0.72$ ), which can be attributed to the reduction of [Fe<sup>MeCN</sup>]<sup>+</sup>. The second reversible reduction system observed in MeCN at  $E_{1/2} = -0.82$  V ( $\Delta E_p = 110$  mV) disappears after addition of [LutH]<sup>+</sup>, and can be attributed to the reduction of the dinuclear Fe<sup>III</sup>-hydroxo side product [Fe<sub>2</sub><sup>OH</sup>]<sup>+</sup>, that has been detected by <sup>1</sup>H NMR and ESI-MS in acetonitrile (see above). It should be noted that the peak corresponding to the reduced species of [Fe<sub>2</sub><sup>SS</sup>]<sup>2+</sup>, which was also detected in the NMR spectrum in CD<sub>3</sub>CN, is not observed in this CV. Consequently, we can propose a fast equilibrium (in the CV timescale) between [Fe<sub>2</sub><sup>SS</sup>]<sup>2+</sup> and [Fe<sup>MeCN</sup>]<sup>+</sup> that precedes the one-electron reduction of [Fe<sup>MeCN</sup>]<sup>+</sup> (while [Fe<sub>2</sub><sup>SS</sup>]<sup>2+</sup> is not directly reduced).

The overall data are thus consistent with the fact that the solid state isolated Fe<sup>II</sup>-disulfide complex [Fe<sub>2</sub><sup>SS</sup>]<sup>2+</sup> remains stable in solution in non-coordinating CH<sub>2</sub>Cl<sub>2</sub>, while it partly or

fully converts into a mononuclear Fe<sup>III</sup>-thiolate solvent adduct, [Fe<sup>Solv</sup>]<sup>+</sup>, in coordinating solvents (see Scheme 3). This process corresponds to an intramolecular electron transfer that involves concomitantly the oxidation of the two Fe<sup>II</sup> ions to Fe<sup>III</sup> and the reduction of the bridging disulfide into two terminal Fe-bound thiolates.

**Halide-dependent thiolate/disulfide interconversion.** With the objective of interconverting Fe<sup>II</sup>-disulfide and Fe<sup>III</sup>-thiolate complexes in a controlled manner, addition of halide co-ligands to [Fe<sub>2</sub><sup>SS</sup>]<sup>2+</sup> and their subsequent removal seems to be a convenient strategy,<sup>[8]</sup> especially since the [Fe<sup>III</sup>(LS)X] (Fe<sup>X</sup>, X = Cl, I) complexes have been already isolated and described.<sup>[15-16]</sup> This investigation has been carried out in CH<sub>2</sub>Cl<sub>2</sub>, wherein the Fe<sup>II</sup>-disulfide form of the complex ([Fe<sub>2</sub><sup>SS</sup>]<sup>2+</sup>) is the only stable form in the absence of halides (see previous paragraph). In the presence of ~2 equivalents of Et<sub>4</sub>NCl, the colour of a CH<sub>2</sub>Cl<sub>2</sub> solution of [Fe<sub>2</sub><sup>SS</sup>]<sup>2+</sup> changes immediately from yellow to pinkish brown in less than 5 seconds (Figure 7a). The UV-vis spectrum of this species corresponds to the [Fe<sup>III</sup>(LS)Cl] complex (Fe<sup>Cl</sup>).<sup>[15]</sup> Based on the extinction coefficient of the intense transition at 495 nm determined in CH<sub>2</sub>Cl<sub>2</sub> ( $\epsilon \approx 7200 \text{ L}\cdot\text{mol}^{-1}\cdot\text{cm}^{-1}$ ) we conclude that the reaction is not only rapid but also quantitative. The feasibility of the reversible reaction has been investigated. After the addition of ~1 equivalent of Li[B(C<sub>6</sub>F<sub>5</sub>)<sub>4</sub>]<sub>2</sub>.5Et<sub>2</sub>O to a CH<sub>2</sub>Cl<sub>2</sub> solution of Fe<sup>Cl</sup>, [Fe<sub>2</sub><sup>SS</sup>]<sup>2+</sup> is regenerated quantitatively in 10 minutes (Figure 7b), evidencing the reversibility of the transformation. This chemical interconversion can be repeated at least three times on the same sample without significant loss of efficiency. As expected, Fe<sup>Cl</sup> can be also quantitatively generated by addition of ~1 equiv. of Et<sub>4</sub>NCl to a DMF solution of [Fe<sup>DMF</sup>]<sup>+</sup> (Figure S5).

The role of the halide nature in triggering the Fe<sup>II</sup>-disulfide/Fe<sup>III</sup>-thiolate interconversion process was investigated. After the addition of two equivalents of *n*-Bu<sub>4</sub>NI into a CH<sub>2</sub>Cl<sub>2</sub> solution of [Fe<sub>2</sub><sup>SS</sup>]<sup>2+</sup>, the UV-vis spectrum displays three absorption bands at 516 nm, 630 nm and 770 nm (Figure S3a), he corresponding to [Fe<sup>III</sup>(LS)I] (Fe<sup>I</sup>).<sup>[16]</sup> Based on the absorption properties of Fe<sup>I</sup>, it can be concluded that the reaction is still quantitative and fast (about 10 seconds) as for Fe<sup>Cl</sup>. However, the reverse process is only partial and requires the presence of a large excess (20 equiv.) of Li[B(C<sub>6</sub>F<sub>5</sub>)<sub>4</sub>]<sub>2</sub>.5Et<sub>2</sub>O (Figure S3b).

In the attempt of rationalization of the [Fe<sub>2</sub><sup>SS</sup>]<sup>2+</sup>/Fe<sup>X</sup> interconversion process, the redox properties of Fe<sup>X</sup> (X = Cl, I) have been investigated (in CH<sub>2</sub>Cl<sub>2</sub> solution, Figure 8) and compared with those of [Fe<sub>2</sub><sup>SS</sup>]<sup>2+</sup>. While the CV of Fe<sup>I</sup> displays a poorly reversible reduction process at  $E_{pc} = -0.86 \text{ V}$  vs Fc/Fc<sup>+</sup> ( $E_{pa} = -0.72 \text{ V}$ ,  $ip_a/ip_c = 0.59$ ), the electron transfer becomes fully reversible for Fe<sup>Cl</sup> at  $E_{1/2} = -0.92 \text{ V}$  ( $\Delta E_p = 99 \text{ mV}$ ,  $ip_a/ip_c = 0.93$ ). In both systems, this signal is assigned to the one electron reduction of the Fe<sup>III</sup> ion to Fe<sup>II</sup>. In the latter case, the metal-based reduction process has been unambiguously confirmed by the structure of the one-electron reduced form of Fe<sup>Cl</sup>, [Fe<sup>Cl</sup>]<sup>-</sup> (see above).

## Discussion

The  $[\text{Fe}_2^{\text{SS}}]^{2+}$  complex shows solvent-dependent properties: while in non-coordinating  $\text{CH}_2\text{Cl}_2$ ,  $[\text{Fe}_2^{\text{SS}}]^{2+}$  is the only stable form, in the presence of coordinating solvents like MeCN or DMF, it is partly or fully converted into mononuclear  $\text{Fe}^{\text{III}}$ -thiolate species having a bound solvent molecule ( $[\text{Fe}^{\text{Solv}}]^+$ ). In DMF the equilibrium lies far on the adduct ( $[\text{Fe}^{\text{DMF}}]^+$ ) side, while both  $[\text{Fe}^{\text{MeCN}}]^+$  and  $[\text{Fe}_2^{\text{SS}}]^{2+}$  are present in MeCN. The affinity of the coordinating solvent for iron(III) ( $\text{DMF} > \text{MeCN}$ ) seems thus to be crucial to control the (inter)conversion process. Solvent dependency for  $\text{M}^{\text{n}}$ -disulfide/ $\text{M}^{\text{n+1}}$ -thiolate (inter)conversion has been previously reported only in the case of a dicopper complex. In that case, both the nature of the solvent and the temperature allowed the control of the equilibrium in favour of one of these species.<sup>[5-6]</sup> However, differently from the present case, the  $\text{Cu}^{\text{I}}$ -disulfide/ $\text{Cu}^{\text{II}}$ -thiolate interconversion process was driven by solvent polarity and not by its coordinating properties. As a result, the  $\text{Cu}^{\text{I}}$ -disulfide species was preferably formed in polar solvents,<sup>[5]</sup> while the formation of the present  $\text{Fe}^{\text{II}}$ -disulfide complex is promoted in apolar solvents. This demonstrates that the effect of the solvent is system-dependent and no general conclusion can be drawn. In the absence of halides, in the cases of the Co and Mn complexes isostructural to  $[\text{Fe}_2^{\text{SS}}]^{2+}$ , the corresponding  $\text{M}^{\text{III}}$ -thiolate forms could not be observed (for  $[\text{Co}_2^{\text{SS}}]^{2+}$ <sup>[8a]</sup>) nor stabilized (in the case of  $[\text{Mn}_2^{\text{SS}}]^{2+}$ <sup>[8b]</sup>) in any solvent. All these data highlight how the nature of the metal has a drastic effect on the  $\text{M}^{\text{n}}$ -disulfide/ $\text{M}^{\text{n+1}}$ -thiolate interconversion process. A  $\text{Mn}^{\text{III}}$ -thiolate complex could only be detected as a transient species towards the irreversible formation of the  $\text{Mn}^{\text{II}}$ -disulfide complex ( $[\text{Mn}_2^{\text{SS}}]^{2+}$ ) during the electrochemical oxidation of the  $\text{Mn}^{\text{II}}$  precursor. In our previous study, this species was assigned to a dinuclear thiolate-bridged  $\text{Mn}^{\text{III}}$  species ( $[\text{Mn}_2]^{2+}$ ).<sup>[8b]</sup> However, because the redox properties of the Fe- and Mn- systems are comparable, it cannot be excluded that this  $\text{Mn}^{\text{III}}$ -thiolate complex is a mononuclear  $\text{Mn}^{\text{III}}$ -MeCN adduct ( $[\text{Mn}^{\text{MeCN}}]^+$ ) similar to  $[\text{Fe}^{\text{MeCN}}]^+$ .

We have previously shown for the parent Co- and Mn-based complexes,<sup>[8]</sup> that the  $\text{M}^{\text{II}}$ -disulfide/ $\text{M}^{\text{III}}$ -thiolate interconversion process can be controlled by (de)coordination of halide anions. To investigate the role of the metal in this halide-mediated process, the reactivity of the disulfide Fe complex with chloride and iodide was explored. While the conversion from the  $\text{Fe}^{\text{II}}$ -disulfide to the  $\text{Fe}^{\text{III}}$ -thiolate species is quantitative and fast in the presence of  $\text{X} = \text{Cl}$  or  $\text{I}$ , the removal of the halide with  $\text{Li}[\text{B}(\text{C}_6\text{F}_5)_4] \cdot 2.5\text{Et}_2\text{O}$  leads to the slow but quantitative formation of the  $\text{Fe}^{\text{II}}$ -disulfide complex for  $\text{X} = \text{Cl}$ , and only to marginal reaction for  $\text{X} = \text{I}$ . It thus appears that the behaviour of the Fe switch is just in between to that of the Co switch (fast and quantitative conversion in both directions) and that of the Mn-based system (slow and only partial disulfide to thiolate conversion).

The efficiency of the Fe-based switch controlled by the addition/removal of halides, and to a lesser extent by the nature of the solvent, can be rationalized from the redox properties of the involved complexes, which are directly related to the electronic density distribution between the metal and the sulfur atoms. In the absence of halide, the small reduction potential

difference between the Fe<sup>III</sup>-thiolate and the Fe<sup>II</sup>-disulfide forms ( $E_{pc} = -0.62$  or  $-0.75$  V vs Fc<sup>+</sup>/Fc for [Fe<sup>Solv</sup>]<sup>+</sup>, Solv = MeCN or DMF, respectively, and  $-0.84$  V for [Fe<sub>2</sub><sup>SS</sup>]<sup>2+</sup>) agrees with the fact that both species can be stabilized by tuning the experimental conditions. In the case of the parent Mn compounds, the reduction potential difference was much higher, with the Mn<sup>II</sup>-disulfide form being much more difficult to reduce ( $E_{pc} = -1.17$  V for [Mn<sub>2</sub><sup>SS</sup>]<sup>2+</sup> vs  $E_{pc} = -0.47$  V for [Mn<sub>2</sub>]<sup>2+</sup> ([Mn<sup>MeCN</sup>]<sup>+</sup>)). These results are coherent with the fact that the Mn<sup>III</sup> thiolate complex slowly but irreversibly evolves in solution to [Mn<sub>2</sub><sup>SS</sup>]<sup>2+</sup>, while the [Fe<sup>MeCN</sup>]<sup>+</sup> and [Fe<sub>2</sub><sup>SS</sup>]<sup>2+</sup> forms can coexist in equilibrium.

In the presence of halide, one condition for an efficient M<sup>II</sup>-disulfide to M<sup>III</sup>-thiolate conversion to occur is that the reduction potential of the M<sup>X</sup>/ [M<sup>X</sup>]<sup>-</sup> couple is lower or similar to that of the corresponding [M<sub>2</sub><sup>SS</sup>]<sup>2+</sup>/ M<sub>2</sub> pair (M<sub>2</sub> = [M<sup>II</sup><sub>2</sub>(LS)<sub>2</sub>], i.e. the two-electron reduced form of [M<sub>2</sub><sup>SS</sup>]<sup>2+</sup>). This is the case of the Fe-based system, for which the generated mononuclear Fe<sup>X</sup> (X = Cl, I) complexes are less easily reduced ( $E_{1/2} = -0.92$  V and  $E_{pc} = -0.86$  V vs Fc<sup>+</sup>/Fc for X = Cl and I, respectively) compared to [Fe<sub>2</sub><sup>SS</sup>]<sup>2+</sup> ( $E_{pc} = -0.84$  V). This is also the case for the Co system but not for the Mn-based one, for which the Mn<sup>II</sup>-disulfide form, [Mn<sub>2</sub><sup>SS</sup>]<sup>2+</sup>, is much more difficult to reduce. The trend of  $E_{pc}$  values for the [M<sub>2</sub><sup>SS</sup>]<sup>2+</sup> complexes (Mn << Fe < Co, Table 2) is directly correlated with the stability of the S-S bond (Mn >> Fe > Co). This is most likely due to the decrease in the covalent character of the M-S<sub>S-S</sub> bond from cobalt to manganese, iron being an intermediate case.<sup>[20]</sup>

Concerning the reverse process, i.e. the M<sup>III</sup>-thiolate to M<sup>II</sup>-disulfide conversion, the ability for this reaction to occur is at a lower reduction potential of [M<sub>2</sub><sup>SS</sup>]<sup>2+</sup> with respect to the corresponding M<sup>III</sup>-thiolate species as is the case of both the Fe and Mn systems (Table 2). However, other factors can affect the process. As an example, the difference of reactivity between Fe<sup>Cl</sup> and Fe<sup>I</sup> can be explained by the different solubility in CH<sub>2</sub>Cl<sub>2</sub> of the LiX salts co-generated during the anion exchange process (LiI being more soluble than LiCl). Concerning the Co system, this conversion is too fast to observe the transient formation of Co<sup>III</sup> species (as [Co<sub>2</sub>]<sup>2+</sup> or [Co<sup>MeCN</sup>]<sup>+</sup>), indicating that the redox potential of [Co<sub>2</sub><sup>SS</sup>]<sup>2+</sup> is much lower.

## Conclusion

In M<sup>n+</sup>-disulfide/M<sup>(n+1)+</sup>-thiolate interconverting systems, the nature of the metal notably modulates the redox properties of the sulfur-based ligand by controlling its electronic structure. Our data collected on a series of closely related Fe-, Mn- and Co-based systems evidence how the efficiency of this interconversion relies on the fine-tuning of the redox properties of the different complexes involved, and on the nature of the M-S bond for the different metal ions. However, these properties are difficult to predict: even if trends can be extracted, the analysis remains qualitative. Amongst the three different switches, the Fe system is the only one displaying Fe<sup>II</sup>-disulfide / Fe<sup>III</sup>-thiolate (inter)conversion controlled by the coordinating abilities of the solvent and not just by addition/removal of halides.

Thiolate/disulfide interconversion processes mediated by a metal ion has been previously proposed only in the case of copper for different biological purposes including copper delivery and protection of cells against reactive oxygen species (ROS). From the present study, it can be anticipated that a similar reactivity can be mediated by iron in the suitable ligand environment especially by considering that it is the main metal at the origin of the formation of ROS via the Fenton reaction.

## Experimental part

*General.* The syntheses of  $[\text{Fe}^{\text{III}}_2(\text{LS})_2(\mu\text{-O})]$  ( $\text{Fe}_2^{\text{O}}$ ) and of  $[\text{Fe}^{\text{III}}(\text{LS})\text{X}]$  ( $\text{X} = \text{Cl}$ ,  $\text{Fe}^{\text{Cl}}$  and  $\text{X} = \text{I}$ ,  $\text{Fe}^{\text{I}}$ ) were previously reported.<sup>[15-16]</sup> All reactions were carried out under an atmosphere of dry nitrogen (glove box). The elemental analyses were carried out with a CHN analyser (SCA, CNRS). The ESI-MS spectra were recorded on an amaZon speed and TQ QUATTRO II ion trap spectrometers equipped with an electrospray ion source (ESI). The samples were analysed in positive ionization mode by direct perfusion in the ESI-MS interface. The infrared spectra were registered on a Magna-IR TM 550 Nicolet spectrometer as KBr pellets. Electronic absorption spectra were recorded on a ZEISS MCS 601 UV-NIR photodiode-array spectrophotometer. The  $^1\text{H}$  NMR spectra have been recorded on a Bruker Avance III 500 MHz spectrometer using standard Bruker pulse sequence. Longitudinal relaxation time (T1) measurements have been carried out by using standard inversion recovery sequence. Magnetic susceptibility measurements in solution have been performed by the Evans method.<sup>[18]</sup> Cw X-band EPR spectra were recorded on a Bruker EMX, equipped with the ER-4192 ST Bruker cavity and an ER-4131 VT at 100 K.

*Synthesis of  $[\text{Fe}^{\text{II}}_2(\text{LSSL})](\text{ClO}_4)_2$  ( $[\text{Fe}^{\text{SS}}](\text{ClO}_4)_2$ ).* A MeCN solution of  $\text{HClO}_4$  (60  $\mu\text{L}$ , 1 M, 0.06 mmol) was added to a suspension of  $[\text{Fe}^{\text{III}}_2(\text{LS})_2(\mu\text{-O})]$  (20 mg, 0.016 mmol) in MeCN (4 mL) at room temperature. The reaction mixture was stirred over 20 min to give a dark brown solution in 20 min. The volume was reduced to 2 mL and then  $\text{Et}_2\text{O}$  (8 mL) was slowly added. An orange-red precipitate was formed after standing the resulting mixture overnight. The precipitate was isolated by filtration, washed by MeCN and dried ( $[\text{Fe}^{\text{SS}}](\text{ClO}_4)_2$ , 10.1 mg, 0.007 mmol, 44%). IR ( $\text{cm}^{-1}$ ): 3101(w), 3058(m), 2962(m), 2933(m), 2876(m), 1598(m), 1569(m), 1490(m), 1479(m), 1465(m), 1443(m), 1383(w), 1328(w), 1274(w), 1210(w), 1189(w), 1158(w), 1077(vs), 1035(s), 1015(s), 999(m), 957(m), 919(m), 845(w), 835(w), 807(m), 791(w), 749(m), 738(m), 693(s), 656(m), 647(w), 634(m), 621(s), 596(m), 587(m), 575(w), 566(w), 524(w), 517(w), 506(s). Anal. Calcd for  $\text{C}_{76}\text{H}_{60}\text{N}_4\text{S}_4\text{Fe}_2\text{Cl}_2\text{O}_8 \cdot 2(\text{CH}_3\text{CN}) \cdot 2\text{H}_2\text{O}$ : C, 60.57; H, 4.45; N, 5.30. Found: C, 60.33; H, 4.27; N, 5.45. X-ray suitable deep orange block single crystals corresponding to  $[\text{Fe}^{\text{SS}}](\text{ClO}_4)_2 \cdot 2\text{CH}_3\text{CN}$  were obtained by slow diffusion of diethyl ether onto a small fraction

of acetonitrile reaction solution.

*Synthesis of  $[Fe^{III}(LS)(DMF)]ClO_4$  ( $[Fe^{DMF}]ClO_4$ ).* Diethyl ether was slowly diffused onto a DMF solution (3 mL) of  $[Fe^{SS}](ClO_4)_2$  (15 mg, 0.010 mmol) at 293 K. After one week, black block X-ray suitable single crystals were obtained, corresponding to  $[Fe^{DMF}]ClO_4 \cdot 2DMF \cdot 0.5Et_2O$  (8.0 mg, 0.008 mmol, 80%). IR ( $cm^{-1}$ ): 2292(vs), 2852(vs), 1660(s), 1632(s), 1600(s), 1569(m), 1487(s), 1468(s), 1442(s), 1424(m), 1264(m), 1208(w), 1185(m), 1157(m), 1101(s), 1082(s), 1025(m), 1017(m), 1000(w), 809(m), 792(s), 753(m), 746(s), 695(vs), 665(s), 650(s), 619(m), 612(m), 606(m), 599(vs), 589(m), 586(w), 583(w), 575(w), 566(m), 559(w), 553(w).

*Crystallization of  $[CoCp_2][Fe^{II}(LS)Cl]$  ( $[CoCp_2][Fe^{Cl}]$ ).* A MeCN solution (2 ml) of cobaltocene ( $CoCp_2$ , 2.83 mg, 0.015 mmol) was added to a suspension of  $Fe^{Cl}$  (10 mg, 0.015 mmol) in MeCN (2 mL). The light purple reaction mixture quickly turned to a green solution. After stirring for 1 h, the solution was filtered and diethyl ether was slowly diffused onto it at 293 K. After few days, X-ray suitable dark green single crystals were obtained, corresponding to  $[CoCp_2][Fe^{Cl}] \cdot 0.5MeCN$ .

*X-ray Crystallography.* Crystallographic data and selected bond lengths and angles for  $[Fe^{II}_2(LSSL)](ClO_4)_2 \cdot 2CH_3CN$  (CCDC 1579778),  $[Fe^{III}(LS)(DMF)]ClO_4 \cdot 2DMF \cdot 0.5Et_2O$  (CCDC 1828212), and  $[CoCp_2][Fe^{III}(LS)Cl]$  (CCDC 1579779) are tabulated in Tables S1 and S2. Single-crystal diffraction data were measured on a Bruker-AXS-Enraf-Nonius Kappa diffractometer with an APEXII area detector and an Incoatec high brilliance microfocus source (MoK $\alpha$  radiation, Multilayers mirrors monochromator,  $\lambda$  0.71073Å) at 200 K. The OLEX2 program package was used for cell refinements and data reductions.<sup>[21]</sup> An absorption correction (SADABS) was applied to the data. Molecular structures were solved by charge flipping and refined on F2 by full matrix least-squares techniques, using the SHELXTL package.<sup>[22]</sup> All non-hydrogen atoms were refined anisotropically and all hydrogen atoms were placed at their calculated positions.

*Mössbauer spectroscopy.* Mössbauer spectra were recorded with a  $^{57}Co$  source in a Rh matrix using an alternating constant acceleration Wissel Mössbauer spectrometer operated in the transmission mode and equipped with a Janis closed-cycle helium cryostat. The isomer shift is given relative to iron metal at ambient temperature. Simulation of the experimental data was performed with the Mfit program using Lorentzian line doublets (E. Bill, Max-Planck Institute for Chemical Energy Conversion, Mülheim/Ruhr, Germany. E-mail: [eckhard.bill@cec.mpg.de](mailto:eckhard.bill@cec.mpg.de); webpage: <http://www.cec.mpg.de/research/molecular-theory-and-spectroscopy/moessbauer-mcd.html?L=1>).

*Electrochemical measurements.* *n*-Tetrabutylammonium perchlorate ( $Bu_4NClO_4$ ) was used as

received and stored in glove box. DMF (99.8 %, extra dry), MeCN (99.99%) and CH<sub>2</sub>Cl<sub>2</sub> (99.99%) were degassed with argon prior to use. Electrochemical experiments were performed under argon in a glove box with less than 5 ppm of O<sub>2</sub> by using a PGSTAT100N Metrohm potentiostat/galvanostat. A standard three-electrode electrochemical cell was used. Potentials were referenced to an Ag/0.01M AgNO<sub>3</sub> electrode in CH<sub>3</sub>CN / 0.1 M Bu<sub>4</sub>NClO<sub>4</sub> and measured potentials were calibrated through the use of an internal Fc<sup>+</sup>/Fc standard. The working electrode was a vitreous carbon disk (3 mm in diameter) polished with 2 mm diamond paste (Mecaprex Presi) for cyclic voltammetry ( $E_{pa}$  = anodic peak potential;  $E_{pc}$  = cathodic peak potential). The auxiliary electrode was a Pt wire in CH<sub>3</sub>CN / 0.1 M Bu<sub>4</sub>NClO<sub>4</sub>.

*Theoretical calculations.* We utilized the density functional theory (DFT) method B3LYP<sup>[23]</sup> for geometry optimizations of dinuclear [Fe<sub>2</sub>]<sup>2+</sup>, [Fe<sub>2</sub>O] and [Fe<sup>SS</sup>]<sup>2+</sup> complexes as well as conjugated monomers with solvent bound, i.e. [Fe<sup>MeCN</sup>]<sup>+</sup> and [Fe<sup>DMF</sup>]<sup>+</sup> and other related small molecules (HClO<sub>4</sub>, ClO<sub>4</sub><sup>-</sup>, H<sub>2</sub>O, CH<sub>3</sub>CN, DMF).<sup>[24]</sup> In all calculations a 6-31G\* basis set was employed on all atoms for geometry optimizations and frequencies, except on the metals where LANL2DZ with ECP was used.<sup>[25]</sup> Further single point corrections were done at the 6-311+G\*<sup>[26]</sup> level of theory on all atoms, with LANL2DZ as ECP on Iron: basis set BS2 including the polarized continuum model with dielectric constant of  $\epsilon = 35.688$ . All calculations were run in Gaussian-09.<sup>[27]</sup> For the mononuclear complexes [Fe<sup>MeCN</sup>]<sup>+</sup>, [Fe<sup>DMF</sup>]<sup>+</sup> and [Fe<sup>III</sup>LS]<sup>+</sup>, their structures were optimized in various spin states (Doublet, Quartet and Sextet). The calculations confirm that the ground spin state is the quartet spin state for the three species in agreement with experimental data available for [Fe<sup>DMF</sup>]<sup>+</sup> and [Fe<sup>MeCN</sup>]<sup>+</sup>.

**Acknowledgments.** Financial support for this work was provided by Labex arcane (ANR-11-LABX-003), the Agence National de la Recherche and the Deutsche Forschungsgemeinschaft (grants no. ANR-16-CE92\_0012\_01 and DFG Me1313/14-1, NiFeMim), the COST Action CM1305 (EcostBio) and the financial support of China Scholarship Council (L.W.). FGCR thanks the Conacyt Mexico for a studentship.

**Table 1.** Selected bond lengths (Å) for  $[\text{Fe}^{\text{SS}}](\text{ClO}_4)_2 \cdot 2\text{CH}_3\text{CN}$ ,  $[\text{Fe}^{\text{DMF}}]\text{ClO}_4 \cdot 2\text{DMF} \cdot 0.5\text{Et}_2\text{O}$  and  $[\text{CoCp}_2][\text{Fe}^{\text{Cl}}] \cdot 0.5\text{CH}_3\text{CN}$ .

	$[\text{Fe}^{\text{SS}}](\text{ClO}_4)_2 \cdot 2\text{CH}_3\text{CN}$	$[\text{Fe}^{\text{DMF}}]\text{ClO}_4$	$[\text{CoCp}_2][\text{Fe}^{\text{Cl}}]$	
Fe1-N1	2.152(2)	2.022(2)	2.210(3)	2.177(3)
Fe1-N2	2.124(2)	2.033(2)	2.196(3)	2.184(3)
Fe1-S1	2.5513(9)	2.2074(9)	2.3554(12)	2.3495(11)
Fe1-S2	2.4131(9)	2.1970(10)	2.3565(10)	2.3874(11)
Fe1-X <sup>a</sup>	2.3641(10)	2.0164(19)	2.3390(11)	2.3409(11)

<sup>a</sup> X = S2' for  $[\text{Fe}^{\text{SS}}](\text{ClO}_4)_2 \cdot 2\text{CH}_3\text{CN}$ , X = O1 for  $[\text{Fe}^{\text{DMF}}]\text{ClO}_4$  and X = ClA(B) for  $[\text{CoCp}_2][\text{Fe}^{\text{Cl}}]$ .

**Table 2.** Cathodic peak potentials ( $E_{\text{pc}}$ ) in V (vs  $\text{Fc}^+/\text{Fc}$ ) for the  $[\text{M}^{\text{SS}}]^{2+}$ ,  $[\text{M}_2]^{2+}$ ,  $[\text{M}^{\text{MeCN}}]^+$ , and  $\text{M}^{\text{X}}$  (X = Cl or I) complexes (see Scheme S2) determined from CVs recorded in  $\text{CH}_2\text{Cl}_2$  ( $E_{1/2}$  are given in parenthesis for reversible redox systems).

redox system	Co <sup>[8]</sup>	Fe	Mn <sup>[8b]</sup>
$[\text{M}^{\text{SS}}]^{2+}/\text{M}_2$	-0.74	-0.84	-1.17
$[\text{M}_2]^{2+}/\text{M}_2$	nd <sup>a</sup>	-	-0.47 <sup>c</sup>
$2[\text{M}^{\text{MeCN}}]^+/\text{M}_2$	-	-0.75 <sup>b</sup> (-0.71)	-
$\text{M}^{\text{Cl}}/[\text{M}^{\text{Cl}}]^-$	-0.78	-0.96 (-0.92)	nd <sup>a</sup>
$\text{M}^{\text{I}}/[\text{M}^{\text{I}}]^-$	-0.66, -0.74 <sup>d</sup>	-0.86	-0.68

<sup>a</sup>nd: not determined; <sup>b</sup> CV recorded in DMF; <sup>c</sup> CV recorded in MeCN; <sup>d</sup> the reduced species were not unambiguously identified<sup>[8b]</sup>

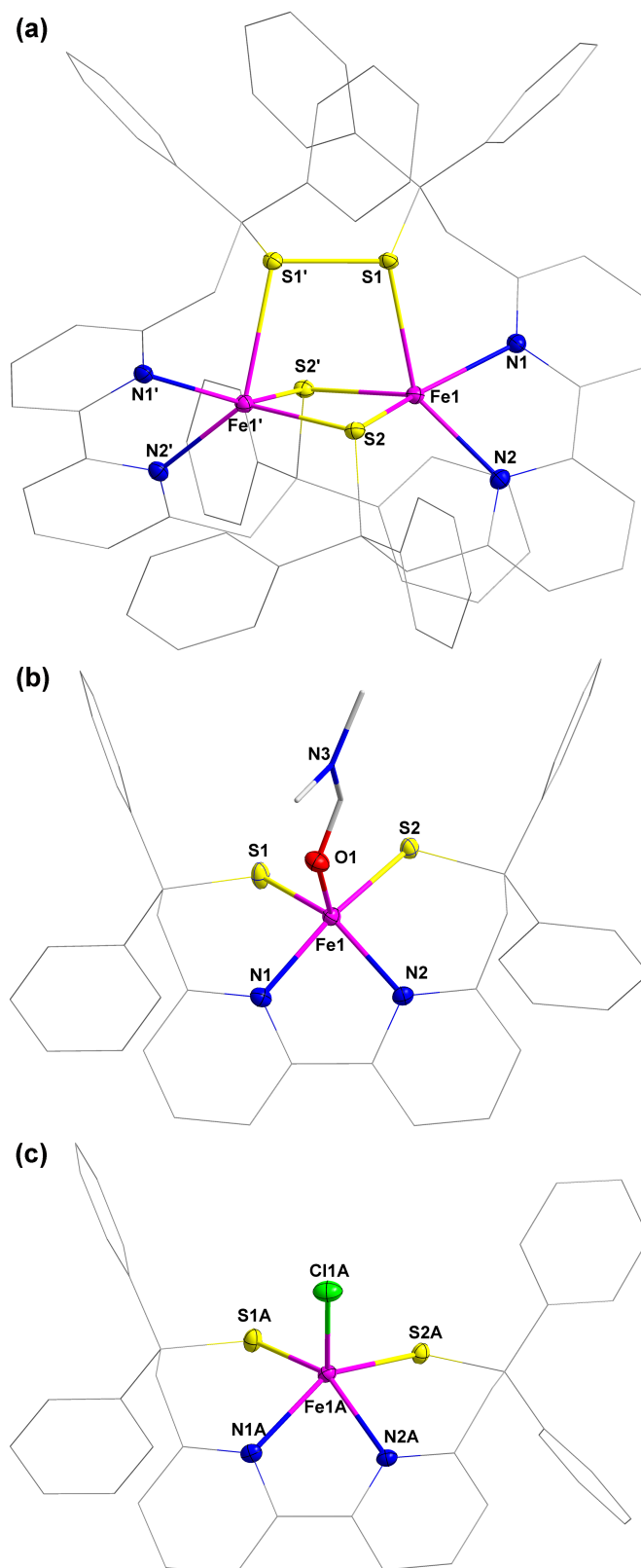


**Figure 1.** Crystal structures of (a)  $[\text{Fe}^{\text{SS}}](\text{ClO}_4)_2$ , (b)  $[\text{Fe}^{\text{DMF}}]\text{ClO}_4$ , and (c)  $[\text{CoCp}_2][\text{Fe}^{\text{Cl}}]$  with partial thermal ellipsoids drawn at 30% probability level. All hydrogen atoms, lattice solvents and counterions are omitted for clarity. For the latter compound, only one of the two independent molecules is shown.

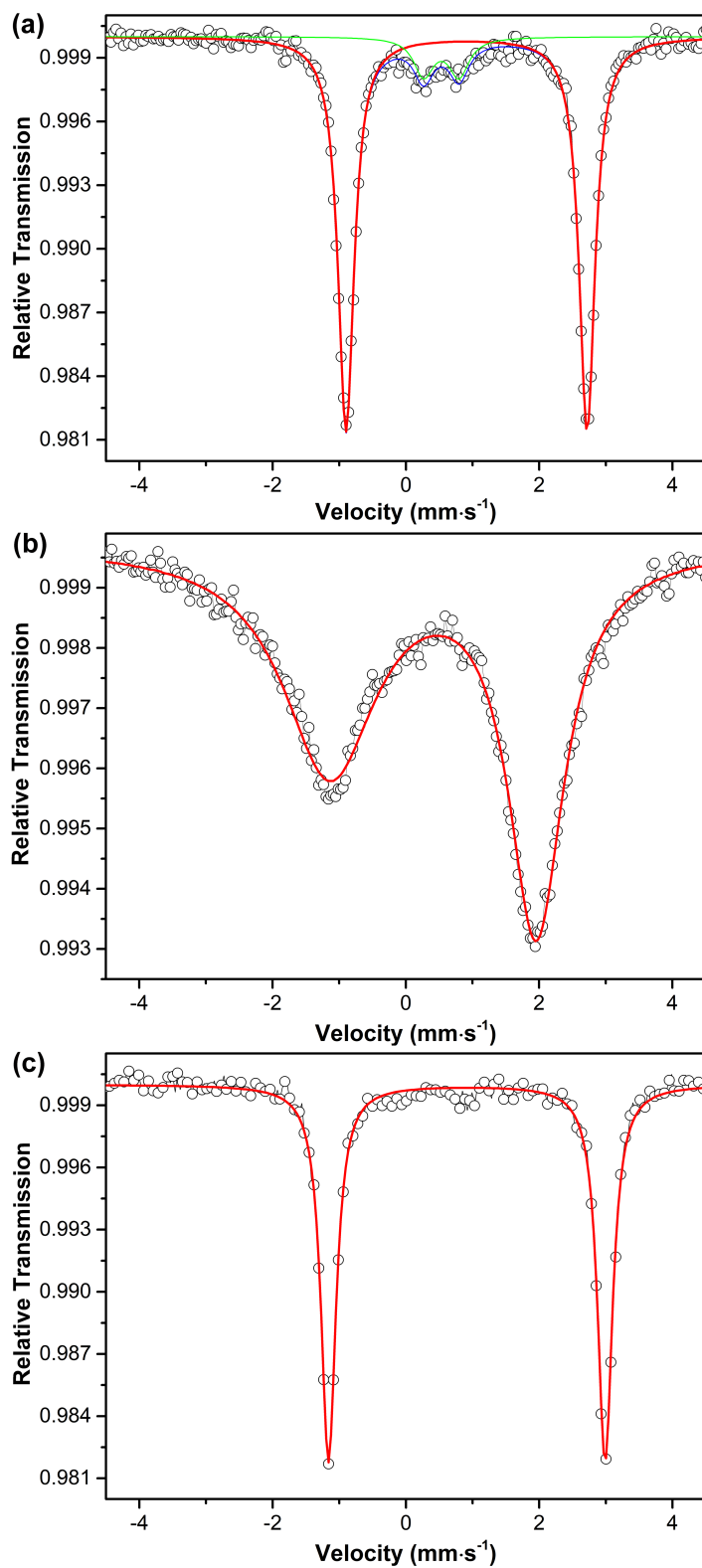


**Figure 2.** Experimental (black empty spots) and simulated (red and green light) zero-field <sup>57</sup>Fe Mössbauer spectra (80 K) of solid (a) [Fe<sup>SS</sup>]<sup>2+</sup>, (b) [Fe<sup>DMF</sup>]<sup>+</sup>, and (c) [Fe<sup>Cl</sup>]<sup>-</sup>.

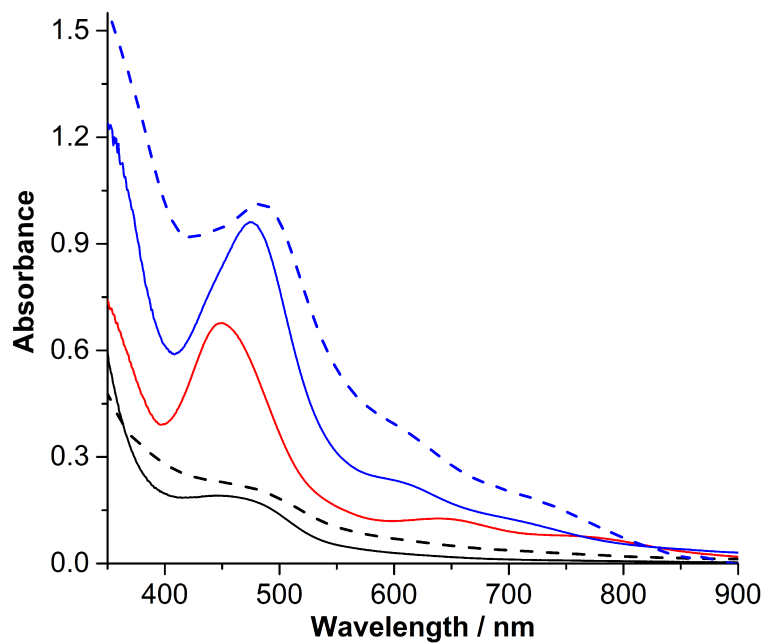


**Figure 3.** UV-vis spectra of  $[\text{Fe}^{\text{SS}}]^{2+}$  in solid state (black dashed,  $\text{NaBF}_4$  pellet) and in solution (0.35 mM, 2 mm path length) of  $\text{CH}_2\text{Cl}_2$  (black), MeCN (red) and DMF (blue). The solid state spectrum of  $[\text{Fe}^{\text{DMF}}]^+$  is also shown for comparison (blue dashed).

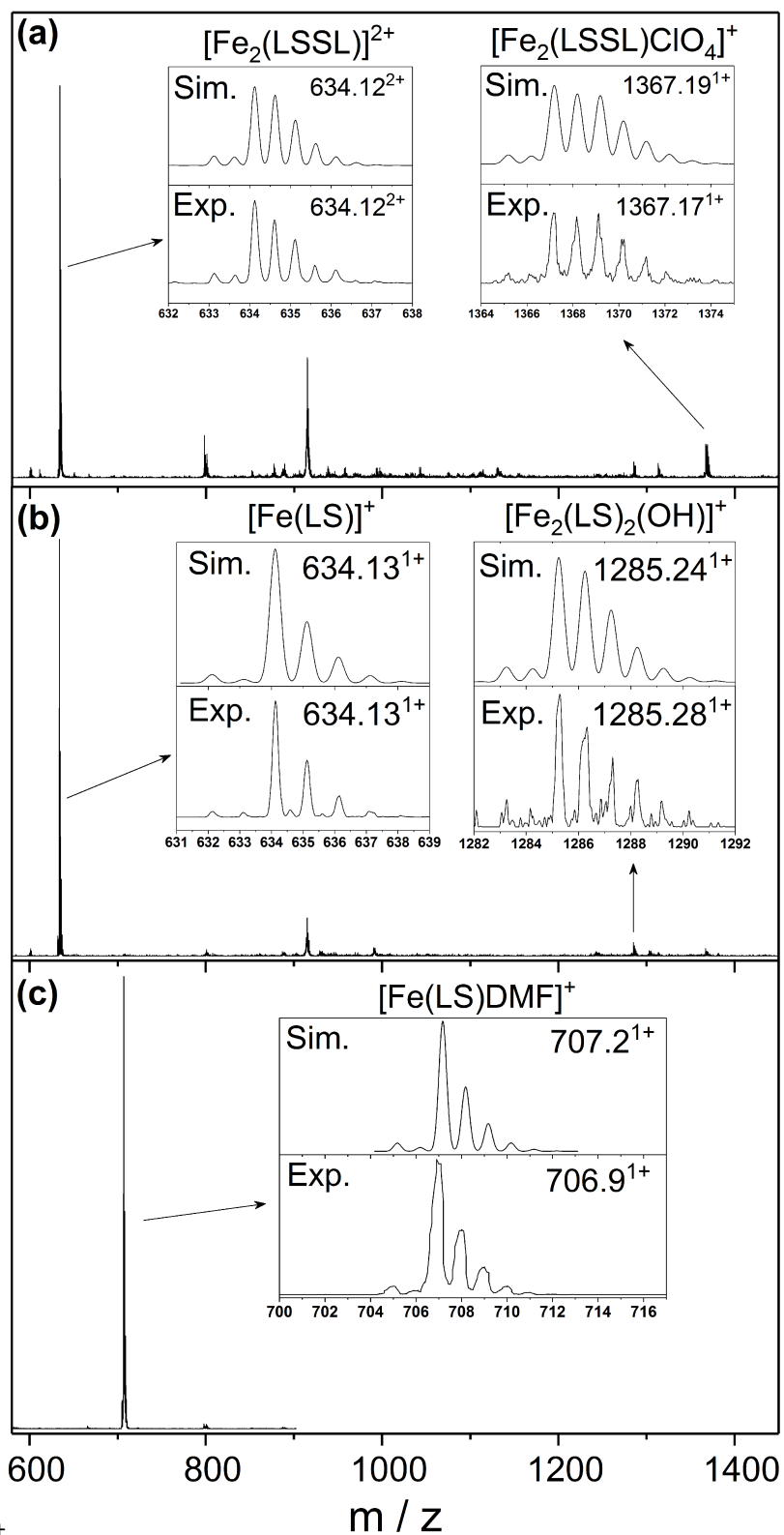


**Figure 4.** ESI-MS spectra of  $[\text{Fe}^{\text{SS}}]^{2+}$  dissolved in (a)  $\text{CH}_2\text{Cl}_2$ , (b) MeCN and (c) DMF. Insets show experimentally obtained (exp.) and simulated (sim.) isotope patterns.

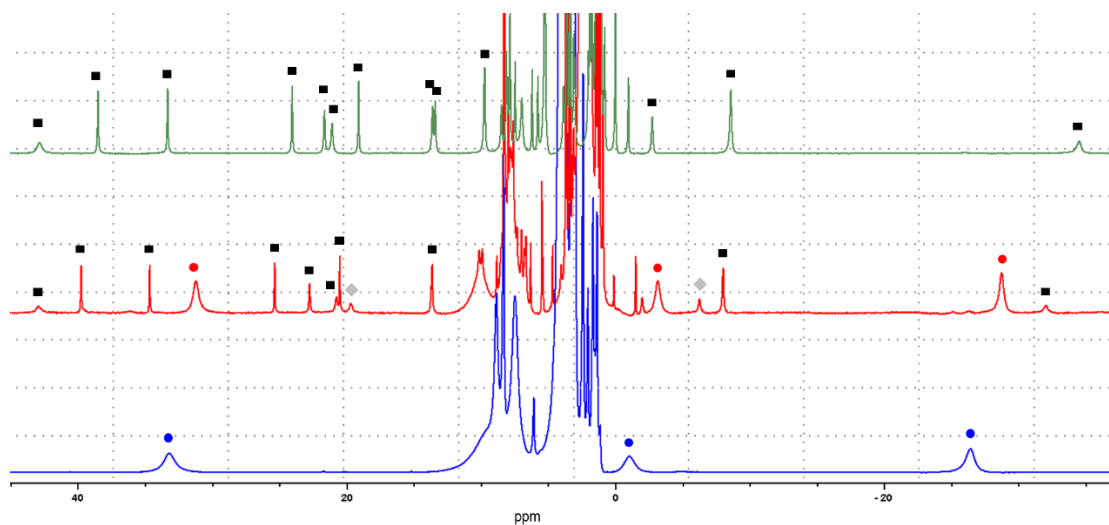


**Figure 5.**  $^1\text{H-NMR}$  spectra of the  $[\text{Fe}_2^{\text{SS}}]^{2+}$  powder dissolved in different solvents:  $\text{CD}_2\text{Cl}_2$  (green),  $\text{CD}_3\text{CN}$  (red),  $\text{d}_7\text{-DMF}$  (blue). Black squares indicate the peaks attributed to the dinuclear  $[\text{Fe}_2^{\text{SS}}]^{2+}$  complex, red and blue circles indicate peaks assigned to mononuclear  $[\text{Fe}^{\text{MeCN}}]^+$  and  $[\text{Fe}^{\text{DMF}}]^+$  species, respectively, while the signals marked with grey diamonds are attributed to an hydroxo-containing/bridged  $\text{Fe}^{\text{III}}$  complex  $[\text{Fe}_2^{\text{OH}}]^{2+}$ .

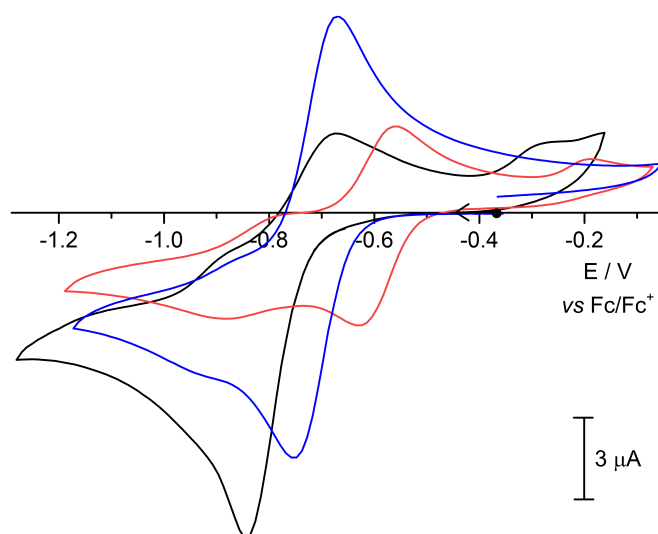


**Figure 6.** CVs of the  $[\text{Fe}_2^{\text{SS}}]^{2+}$  solid dissolved in  $\text{CH}_2\text{Cl}_2$  (black, 0.5 mM), MeCN (red, 0.3 mM), DMF (blue, 0.5 mM). Glassy carbon working electrode,  $100 \text{ mV s}^{-1}$ , 0.1 M  $n\text{-Bu}_4\text{NClO}_4$ .

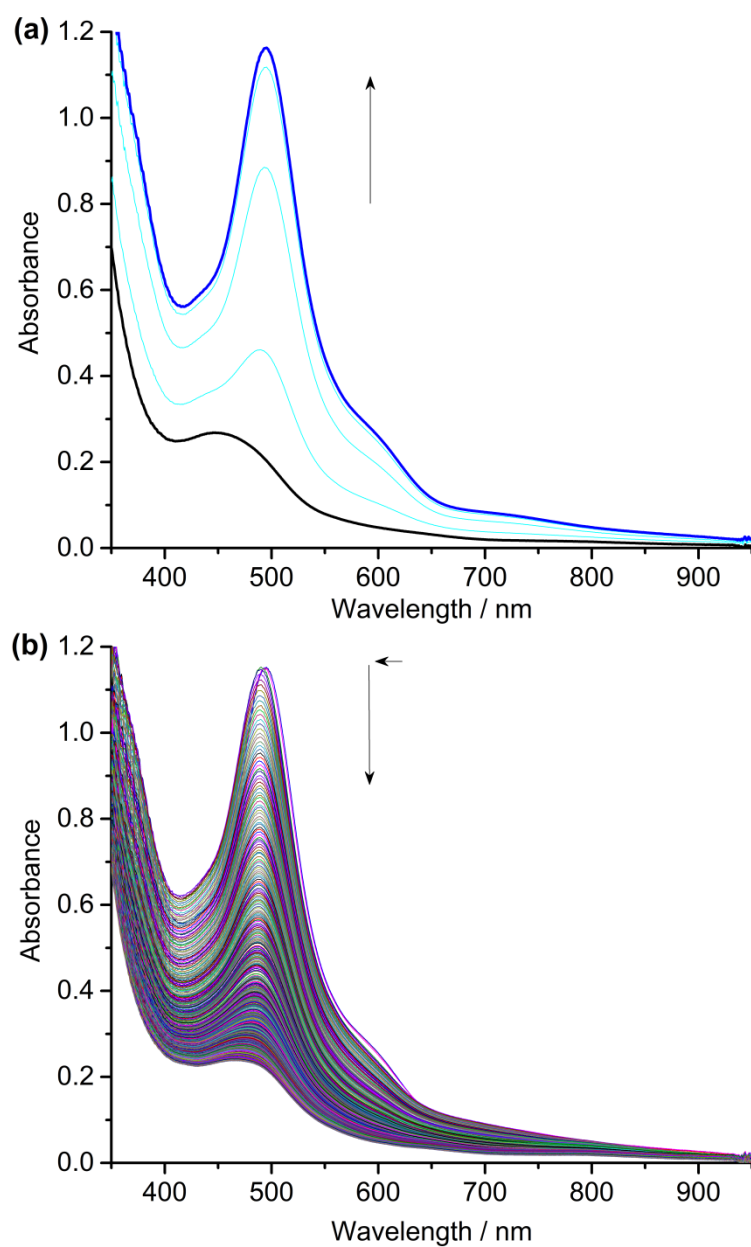


**Figure 7.** UV-vis spectral evolution of (a)  $[\text{Fe}_2^{\text{SS}}]^{2+}$  in  $\text{CH}_2\text{Cl}_2$  (0.1 mM) before and after addition of  $\text{Et}_4\text{NCl}$  (2.1 equiv.) to afford  $\text{Fe}^{\text{Cl}}$ , and (b)  $\text{Fe}^{\text{Cl}}$  (0.2 mM) before and after addition of  $\text{Li}[\text{B}(\text{C}_6\text{F}_5)_4] \cdot 2.5\text{Et}_2\text{O}$  (1.1 equiv.) to recover  $[\text{Fe}_2^{\text{SS}}]^{2+}$  (scan every 1 s, 1 cm path length).

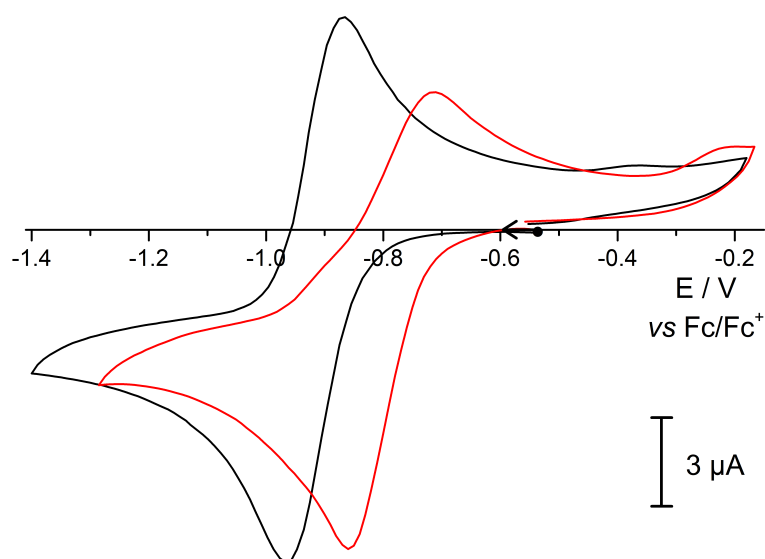


**Figure 8.** CVs of 0.5 mM solutions of  $\text{Fe}^{\text{Cl}}$  (black line) and  $\text{Fe}^{\text{I}}$  (red line) in  $\text{CH}_2\text{Cl}_2$  (glassy carbon working electrode,  $100 \text{ mV s}^{-1}$ ,  $0.1 \text{ M } n\text{-Bu}_4\text{NClO}_4$ ).

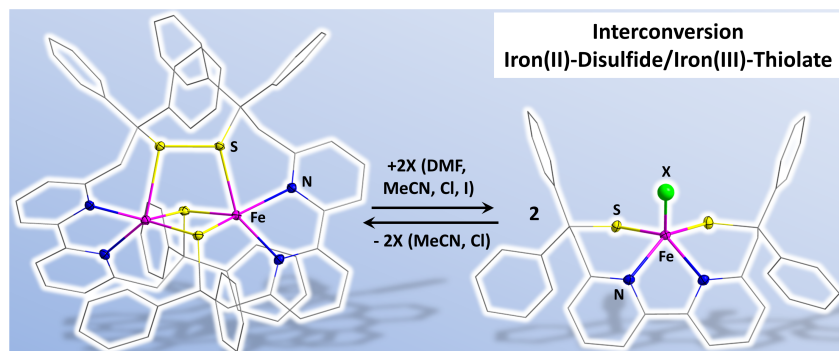
## References

- [1] a) C. E. Paulsen, K. S. Carroll, *Chem. Rev.* **2013**, *113*, 4633-4679; b) T. J. Bechtel, E. Weerapana, *Proteomics* **2017**, *17*, 1600391-n/a; c) Y.-M. Go, D. P. Jones, *Crit. Rev. Biochem. Mol. Biol.* **2013**, *48*, 173-181.
- [2] Y.-M. Go, D. P. Jones, *Biochim. Biophys. Acta* **2008**, *1780*, 1273-1290.
- [3] a) T. R. Cawthorn, B. E. Poulsen, D. E. Davidson, D. Andrews, B. C. Hill, *Biochemistry* **2009**, *48*, 4448-4454; b) B. C. Hill, D. Andrews, *Biochim. Biophys. Acta, Bioenerg.* **2012**, *1817*, 948-954; c) B. P. Dash, M. Alles, F. A. Bundschuh, O. M. H. Richter, B. Ludwig, *Biochim. Biophys. Acta* **2015**, *1847*, 202-211.
- [4] a) K. Jomova, M. Valko, *Toxicology* **2011**, *283*, 65-87; b) J. T. Pedersen, C. Hureau, L. Hemmingsen, N. H. H. Heegaard, J. Østergaard, M. Vašák, P. Faller, *Biochemistry* **2012**, *51*, 1697-1706.
- [5] E. C. M. Ording-Wenker, M. van der Plas, M. A. Siegler, S. Bonnet, F. M. Bickelhaupt, C. Fonseca Guerra, E. Bouwman, *Inorg. Chem.* **2014**, *53*, 8494-8504.
- [6] a) A. M. Thomas, B.-L. Lin, E. C. Wasinger, T. D. P. Stack, *J. Am. Chem. Soc.* **2013**, *135*, 18912-18919; b) E. C. M. Ording-Wenker, M. van der Plas, M. A. Siegler, C. Fonseca Guerra, E. Bouwman, *Chem. Eur. J.* **2014**, *20*, 16913-16921.
- [7] a) A. Neuba, R. Haase, W. Meyer-Klaucke, U. Flörke, G. Henkel, *Angew. Chem. Int. Ed.* **2012**, *51*, 1714-1718; b) Y. Ueno, Y. Tachi, S. Itoh, *J. Am. Chem. Soc.* **2002**, *124*, 12428-12429.
- [8] a) M. Gennari, B. Gery, N. Hall, J. Pécaut, M.-N. Collomb, M. Rouzières, R. Clérac,

- M. Orio, C. Duboc, *Angew. Chem. Int. Ed.* **2014**, *53*, 5318-5321; b) M. Gennari, D. Brazzolotto, S. Yu, J. Pecaut, C. Philouze, M. Rouzieres, R. Clerac, M. Orio, C. Duboc, *Chem. Eur. J.* **2015**, *21*, 18770-18778.
- [9] D. C. Johnson, D. R. Dean, A. D. Smith, M. K. Johnson, *Annu. Rev. Biochem* **2005**, *74*, 247-281.
- [10] W. Lubitz, H. Ogata, O. Rüdiger, E. Reiijerse, *Chem. Rev.* **2014**, *114*, 4081-4148.
- [11] M. Can, F. A. Armstrong, S. W. Ragsdale, *Chem. Rev.* **2014**, *114*, 4149-4174.
- [12] B. M. Hoffman, D. Lukoyanov, Z.-Y. Yang, D. R. Dean, L. C. Seefeldt, *Chem. Rev.* **2014**, *114*, 4041-4062.
- [13] S. J. Dixon, B. R. Stockwell, *Nat. Chem. Biol.* **2014**, *10*, 9-17.
- [14] a) K. H. Hopmann, *Inorganic Chemistry* **2014**, *53*, 2760-2762; b) M. Kayanuma, M. Shoji, M. Yohda, M. Odaka, Y. Shigeta, *The Journal of Physical Chemistry B* **2016**, *120*, 3259-3266.
- [15] M. A. Kopf, D. Varech, J. P. Tuchagues, D. Mansuy, I. Artaud, *J. Chem. Soc., Dalton Trans.* **1998**, 991-998.
- [16] L. Wang, M. Zlatar, F. Vlahović, S. Demeshko, C. Philouze, F. Molton, M. Gennari, F. Meyer, C. Duboc, M. Gruden, *Chem. Eur. J.*, n/a-n/a.
- [17] G. Villar-Acevedo, P. Lugo-Mas, M. N. Blakely, J. A. Rees, A. S. Ganas, E. M. Hanada, W. Kaminsky, J. A. Kovacs, *J. Am. Chem. Soc.* **2017**, *139*, 119-129.
- [18] a) D. F. Evans, *J. Chem. Soc.* **1959**, 2003-2005; b) S. K. Sur, *J. Magn. Reson.* **1989**, *82*, 169-173.
- [19] M. Gennari, D. Brazzolotto, J. Pecaut, M. V. Cherrier, C. J. Pollock, S. DeBeer, M. Retegan, D. A. Pantazis, F. Neese, M. Rouzieres, R. Clerac, C. Duboc, *J. Am. Chem. Soc.* **2015**, *137*, 8644-8653.
- [20] E. I. Solomon, S. I. Gorelsky, A. Dey, *J. Comput. Chem.* **2006**, *27*, 1415-1428.
- [21] O. V. Dolomanov, L. J. Bourhis, R. J. Gildea, J. A. K. Howard, H. Puschmann, *J. Appl. Crystallogr.* **2009**, *42*, 339-341.
- [22] G. M. Sheldrick, SHELXTL-Plus, Structure Determination Software Programs, (Version 6.14.), Bruker Analytical X-ray Instruments Inc., Madison, Wisconsin, USA, **1998**.
- [23] a) A. D. Becke, *Phys. Rev. A* **1988**, *38*, 3098-3100; b) C. T. Lee, W. T. Yang, R. G. Parr, *Phys. Rev. B* **1988**, *37*, 785-789.
- [24] D. Brazzolotto, F. G. Cantú Reinhard, J. Smith-Jones, M. Retegan, L. Amidani, A. S. Faponle, K. Ray, C. Philouze, S. P. de Visser, M. Gennari, C. Duboc, *Angew. Chem. Int. Ed.* **2017**, *56*, 8211-8215.
- [25] P. J. Hay, W. R. Wadt, *J. Chem. Phys.* **1985**, *82*, 270-283.
- [26] R. Krishnan, J. S. Binkley, R. Seeger, J. A. Pople, *J. Chem. Phys.* **1980**, *72*, 650-654.
- [27] R. D. Gaussian 09, M. J. Frisch, G. W. Trucks, H. B. Schlegel, G. E. Scuseria, M. A. Robb, J. R. Cheeseman, G. Scalmani, V. Barone, B. Mennucci, G. A. Petersson, H.

*Nakatsuji, M. Caricato, X. Li, H. P. Hratchian, A. F. Izmaylov, J. Bloino, G. Zheng, J. L. Sonnenberg, M. Hada, M. Ehara, K. Toyota, R. Fukuda, J. Hasegawa, M. Ishida, T. Nakajima, Y. Honda, O. Kitao, H. Nakai, T. Vreven, J. A. Montgomery, Jr., J. E. Peralta, F. Ogliaro, M. Bearpark, J. J. Heyd, E. Brothers, K. N. Kudin, V. N. Staroverov, R. Kobayashi, J. Normand, K. Raghavachari, A. Rendell, J. C. Burant, S. S. Iyengar, J. Tomasi, M. Cossi, N. Rega, J. M. Millam, M. Klene, J. E. Knox, J. B. Cross, V. Bakken, C. Adamo, J. Jaramillo, R. Gomperts, R. E. Stratmann, O. Yazyev, A. J. Austin, R. Cammi, C. Pomelli, J. W. Ochterski, R. L. Martin, K. Morokuma, V. G. Zakrzewski, G. A. Voth, P. Salvador, J. J. Dannenberg, S. Dapprich, A. D. Daniels, Ö. Farkas, J. B. Foresman, J. V. Ortiz, J. Cioslowski, and D. J. Fox, Gaussian, Inc., Wallingford CT, 2009.*

## FULL PAPER



The first disulphide/ thiolate molecular switch based on iron is reported and compared to the parent cobalt- and manganese based systems.

Lianke Wang,<sup>a</sup> Fabian G. Cantú Reinhard,<sup>b</sup> Christian Philouze,<sup>a</sup> Serhiy Demeshko,<sup>c</sup> Sam P. de Visser,<sup>b</sup> Franc Meyer,<sup>c</sup> Marcello Gennari,<sup>a\*</sup> Carole Duboc<sup>a\*</sup>

Page No. – Page No.

Solvent- and halide- induced (inter)conversion between iron(II)-disulfide and iron(III) thiolate complexes.